Evaluation of the Heliosat-4 and FLASHFlux models for solar global daily irradiation estimate in Uruguay

Joaquín Gonzalez[1], Vívian Teixeira[1] and Rodrigo Alonso-Suárez[2]

[1] ITR Centro Sur, Universidad Tecnológica del Uruguay, Durazno (Uruguay)

[2] Facultad de Ingeniería, Universidad de la República, Montevideo, (Uruguay)

Abstract

Solar resource assessment is a fundamental part of solar energy projects risk evaluation. In absence of in-situ measurement or well-calibrated satellite-based estimates, stakeholders tend to rely in freely available solar irradiation data sets, which usually have not been validated against local ground measurements. In this work we provide a performance assessment of Heliosat-4 (CAMS) and FLASHFlux (NASA) solar irradiation models for Uruguay on a daily time scale. It is found that both models present low bias and a rRMSD of 10.0% and 11.6%, respectively, making the former a better option from the end-user perspective. Evidence that the FLASHFlux model overestimate irradiation for coastal oceanic stations is given. The uncertainty obtained for these models is higher than previously locally adjusted satellite-based models, like the modified JPT statistical model, which remain as the best option for the region.

Keywords: solar resource assessment, GHI, Heliosat-4 method, FLASHFlux model.

1. Introduction

In Uruguay, renewable energies have changed the energy landscape. The country has transitioned in less than 10 years from a combination of hydro and fossil fuels supplying the electricity mix to an almost 100% renewable energy mix. The up-to-date figures of Uruguay's generation can be retrieved from the national system operator website (http://adme.com.uy/); for instance, by July 2019 the yearly electricity generation was supplied by 98% of renewable energies, being hydro power 55%, wind power 33%, biomass power 7% and solar power 3%. Hence, only 2% of the supply was provided by fossil fuels thermal generation, mostly used as system back-up for the variable renewable energies short-term intermittency. Solar photovoltaic (PV) generation is gaining in importance and its contribution in the electricity mix is expected to increase significantly in the next decade due to new installations, with a similar expansion as the wind power sector has experienced (Gurín et al., 2018).

The design of solar energy projects requires an accurate solar resource assessment for the project's location (Vignola et al., 2012). The uncertainty of solar resource assessment is directly translated to the financial risk of solar energy ventures and, if high, it can act as an economic barrier for the technology development. In fact, as demonstrated by Schnitzer et al. (2012), the resource uncertainty is the main factor affecting the financial risk of solar energy large-scale PV projects. In the absence of long term controlled quality solar irradiation ground measurements, the industry tends to rely on the available solar satellite estimates, which have not always been validated with local measurements and therefore their uncertainty is unknown. Several models exist to estimate the ground level solar irradiation that make use of satellite images (Perez et al., 2002; Rigollier et al., 2004; Ceballos et al., 2004; Cebecauer et al., 2010; Alonso-Suárez et al., 2012; Kratz et al., 2014; Qu et al., 2017). For areas without snow or high albedo terrain, visible channel images can be used to quantify the cloudiness and then the ground level solar irradiation. These models can be classified in three categories according to their formulation: (i) physical, (ii) statistical and (iii) hybrid. Physical formulations attempt to model in detail the radiative transfer of downward solar irradiance through the atmosphere, and typically require precise information of the atmosphere's state, including clouds properties, aerosols properties, water vapour content, among others, which is not always available with adequate extension and quality. With a few exceptions (Ceballos et al., 2004; Qu et al., 2017), these models are not suitable for operational purpose because they involve calculations that are too computationally expensive for real time operation. Statistical models rely on

empirical relationships between a set of input variables (including satellite information) and the solar irradiation. The parameters of these relationships, which may be parametrizations or machine learning techniques, need to be adjusted using ground measurements. The main disadvantage of this approach is that the coefficients that are tuned for one region shall not be used in others, as the estimates uncertainty can be importantly higher. For a region where high quality ground measurements are not available, it is more suitable to apply a physical approach. The uncertainty of both approaches depends of the characteristics of the site and the quality and availability of the required ground measurements and/or atmospheric information. Hybrids models are in a middle category in where a physical basis is used but some coefficients need to be statistically adjusted to ground measurements. This strategy has been successful in the industry for providing low uncertainty solar irradiation estimates (Perez et al., 2013). At a daily scale, the focus of this work, the typical uncertainties are between 5-15% (as measured by the root mean square deviation relative to the average measurements value) with a low systematic bias between ±5% (as measured by the relative mean bias deviation).

In this work we provide a performance assessment for Uruguay of two publicly available daily solar radiation data sets that are based on physical models that make use of satellite images: the Heliosat-4 method's estimates (Qu et al., 2017) as provided by the Copernicus Atmosphere Monitoring Service (CAMS) and the FLASHFlux model's estimates (Kratz et al., 2014) as provided by the National Aeronautics and Space Administration (NASA). Evaluation is done for the global horizontal irradiation (GHI) using the data as provided by the platforms, without any site adaptation procedure. This is the first performance evaluation of this information in the region at a daily scale. This article is organized as follows. Section 2 describes the ground measurements being used, that are distributed across the Uruguayan territory and are representative of the broader Pampa Húmeda region of the south-east of South America. Section 3 presents the main characteristics of the models being evaluated and the performance metrics that are used for their evaluation. Section 4 presents the results and, finally, Section 5 summarizes our conclusions.

2. Ground measurements

The ground measurements considered in this work were registered in seven sites in Uruguay (see Tab. 1). The data availability time span in each location is different, from three years in the PP site to almost nine years in the LB site. The region is of homogeneous climatic characteristics, with no elevations and mostly plain grassland. The coastal East part of the country is influenced by its proximity to the Atlantic Ocean and is classified as Cfb (temperate, without dry season, warm summers) in the Köppen-Geiger climate classification (Peel et al., 2007). The rest of the country is classified as Cfa (temperate, without dry season, hot summers). The solar irradiation short-term variability of the area is medium and the inter-annual variability is also medium, similar to that of the Central USA (Alonso-Suárez, 2017).

Tab. 1:Details of the measurement stations used in this work.

Site	Code	Lat.(deg)	Lon. (deg)	Alt(m)	Time period used
Canelones	LB	-34.67	-56.34	32	03/2010 - 12/2018
Artigas	AR	-30.40	-56.51	136	01/2012 - 12/2018
Rocha	RC	-34.49	-56.17	24	04/2015 - 10/2018
Colonia	ZU	-34.34	-57.69	81	05/2015 - 10/2018
Salto	LE	-31.28	-57.92	42	10/2015 - 11/2018
Tacuarembó	TA	-31.71	-55.83	140	05/2015 - 10/2018
Treinta y Tres	PP	-33.26	-54.49	58	10/2016 - 12/2018

All the sites in Tab. 1 record the GHI measurements at 1 minute time resolution as an average of 15 seconds samples (4 samples per registered 1 minute value) and use Kipp & Zonen instruments. The LE site is equipped with a Solys2 ground station where the GHI is recorded using a CMP11 Secondary Standard pyranometer. The other six sites correspond to a field measurements network where autonomous stations record the GHI using

CMP6 First Class or CMP10 Secondary Standard pyranometers. All the pyranometers are calibrated every two years against a CMP22 Secondary Standard which is kept with traceability to the Primary Standard in the World Radiation Center.

3. Models and performance

3.l. Models description

The GHI estimates available at the CAMS are generated with the Heliosat-4 method. This method is based on two radiative transfer models, one for clear sky conditions (McClear) and one for cloudy sky conditions (McCloud). Its operational version is based on look-up tables of these models for rapid calculation (Qu et al., 2017; Lefèvre et al., 2013). The model obtains the cloud transmittance and cloud properties from the images of the Meteosat (MSG) geostationary satellite by applying the APOLLO/SEV algorithm, an adaptation of the APOLLO algorithm (Kriebel et al., 2003) for its use with the SEVIRI (Spinning Enhanced Visible and Infrared Imager) instrument in the MSG satellite. The model also integrates advanced products for aerosol, ozone and water vapour estimation for its clear sky modeling. The time and space resolution of the solar estimates follows the MSG satellite capabilities, being available every 15 minutes with an approximate spatial resolution of 7 km for the region under study. The data used here was retrieved on a daily scale directly from SoDa website (http://soda-pro.com/) for the same time period as the ground measurements.

Since the year 2007 the available NASA solar radiation estimates at https://power.larc.nasa.gov/ are based on the FLASHFlux (Fast Longwave and SHortwave radiative Flux) model (Kratz et al., 2014). This model was designed to reduce the processing time in the calculations of the radiation budgets at the surface and at the top of the atmosphere, exchanging some accuracy for speed. It uses the information from the CERES (Clouds and the Earth Radiant Energy System) and MODIS (Moderate Resolution Imaging Spectroradiometer) instruments aboard the Terra and Aqua sun-synchronous orbiting satellites, among other meteorological sources, to estimate the shortwave and longwave radiative fluxes. From January 2008 to date different versions of this model are available at the website: version 2 from 2008 to 2012, version 3AB from 2013 to 2016 and version 3C since 2017. In this work we use GHI measurements (in this context, shortwave downward irradiation) from 2010 to 2018, so the evaluations of this model comprise different versions. In particular, almost all the stations have measurements after 2015, allowing a good performance comparison between the 3AB and 3C FLASHFlux versions. For version 2, only two sites have the adequate time span for its evaluation (AR and LB). The evaluation is done also through the entire measurements time-series as we want to assess the performance of the available information as a whole, from an end-user perspective

3.2. Performance metrics

The performance metrics used for evaluation are the Mean Bias Deviation (MBD), the Root Mean Square Deviation (RMSD) and Kolmogorov-Smirnov Integral (KSI). The first metric measures the systematic bias of the estimates as compared to the measurements while the second one measures the dispersion of the deviations. On the other hand, the KSI metric measures the statistical difference between the estimates and the measurements through all the time-series. This index is based on the two-sample Kolmogorov-Smirnov statistical test to determine if two data sets are statistically similar, hence the metric measures at which extend the estimates and the measurements can be considered as realizations of the same statistical distribution.

The MBD and RMSD are computed as,

$$MBD = \frac{1}{N}\sum_{i=1}^{N}\left(\hat{H}_h - H_h\right),\ RMSD = \sqrt{\frac{1}{N}\sum_{i=1}^{N}\left(\hat{H}_h - H_h\right)^2},$$

where N is the number of days, $\hat{H}_h$ is the estimated daily GHI and H_h is the measured daily GHI, both expressed in MJ/m^2. If the MBD is positive, it means that the estimates are overestimating the data and vice versa if negative. Their relative metrics, rMBD and rRMSD, are expressed as a percentage of the mean measurements value.

The KSI metric is computed by comparing the cumulative distribution functions (CDF) of the estimates and the measurements. If F is the CDF of the measurements and $\hat{F}$ is the CDF of the estimates, then the KSI metric is

defined as the integral of their absolute difference as follows,

$$KSI = \int \left| \hat{F}(H) - F(H) \right| dH$$

The unit for KSI is the same as the daily irradiation H, MJ/m^2.

4. Results

Let us focus first on the MBD and RMSD metrics. The performance for each model in terms of these metrics is shown in Tab. 2 (for all the measurements' period). Results are presented for each station and as an average over all sites (average site performance). In the last row the standard deviation of the metrics is also shown (performance's site variability or geographical variability). The mean bias is small for both models (on average, -0.1% for Heliosat-4 and +0.5% for FLASHFlux). However, when observing each site, the MBD varies approximately between ±2% for both models. The highest rMBD values for the NASA model are positive and are found in the coastal stations of LB and RC (rMBD ≥ +2.0%), which are the closest sites to the Atlantic Ocean. This overestimation phenomenon close to the Atlantic coast was already observed in Alonso-Suárez et al. (2013) for the previous NASA SSE (Surface meteorology and Solar Energy) model. This behavior is not observed for Heliosat-4 method, for which no pattern arises from inspecting the rMBD values. The performance of both models in terms of rRMSD is different: the site average for the Heliosat-4 method is of 10.0% and for the FLASHFlux model is of 11.6%. The geographical variability of the performance is similar for both models and low (less than 1%). Considering both models, the best performance is observed for the AR site (in the North). The scatter plots between the measurements and the estimates for this site are shown in Fig. 1 (a) and (b), for CAMS and NASA models respectively. The overall agreement is good, but a small overestimation bias is observed for the CAMS estimates at low irradiation values. The uncertainty found for these models is higher than locally adjusted models for the region based on GOES-East imagery, which typically have a rMBD between ±1% and a rRMSD of around 7% (Alonso-Suárez et al., 2012).

Tab. 2: Performance indicators for the CAMS and NASA models estimate on a daily basis.

Code	Days	MBD (MJ/m^2)		rMBD (%)		RMSD (MJ/m^2)		rRMSD	
		CAMS	NASA	CAMS	NASA	CAMS	NASA	CAMS	NASA
LB	2779	-0.2	+0.3	-1.4	+2.1	1.6	1.9	9.6	12.0
AR	2153	≈ 0	-0.1	-0.2	-0.5	1.6	1.8	9.1	10.2
RC	1297	+0.3	+0.3	+1.9	+2.0	1.7	1.9	10.9	12.1
ZU	1267	-0.1	+0.1	-0.8	+0.8	1.8	2.0	10.9	12.1
LE	1055	-0.3	-0.2	-1.6	-1.0	1.8	1.9	10.6	11.0
TA	1155	+0.1	+0.1	+0.3	+0.5	1.7	2.0	10.8	12.6
PP	797	≈ 0	-0.1	+0.8	-0.2	1.5	2.0	8.7	11.6
mean	**-**	**≈ 0**	**+0.1**	**-0.1**	**+0.5**	**1.7**	**1.9**	**10.0**	**11.6**
stdev	**-**	**0.2**	**0.2**	**1.3**	**1.2**	**0.1**	**0.1**	**0.9**	**0.8**

Tab. 3 inspects the performance of the FLASHFlux model discriminated by model's version. Due to the measurements time span, the only version that can be evaluated in all stations is the 3C (2017-2018). The 3AB version (2013-2016) can be evaluated in almost all stations with the exception of the PP site, which only has two months of data in the period of this version. The version 2 can only be evaluated in the LB and AR stations, which are the sites with larger data statistic. An overall improvement can be seen in the transition from version 3AB to 3C. The average rMBD is slightly reduced from +0.9% to +0.4%. This overall reduction is not a result of the deviations being lower at each station, rather, some sites increase their rMBD while other reduce it, but as a whole, the average trend is to improve the bias performance. On the other hand, there is an overall rRMSD

reduction from 12.5% to 11.1%. This improvement is significant, and it is consistent across all stations. It can be seen in Tab. 3 that the rRMSD of version 3C is equal or better than the rRMSD of version 3AB in each of the six sites where the comparison can be done. Fig.1 (c) illustrates the rRMSD comparison for these sites. The highest improvements are observed for the ZU, LE and TA stations, with rRMSD increases around 2%. LB and RC stations (the closest sites to the Atlantic Ocean) show almost negligible rRMSD gains, being the rRMSD values approximately the same for both versions. For version 2, the comparison is not conclusive as the amount of sites is reduced. Tab. 3 shows that the MBD is approximately the same in the transition from version 2 to version 3AB. The rRMSD is improved for the LB site but it is downgraded for the AR site.

Tab. 3: Performance comparison between different versions of the FLASHFlux model on a daily basis.

Code	MBD (MJ/m^2)			rMBD (%)			RMSD (MJ/m^2)			rRMSD (%)		
	V2	V3AB	V3C	V2	V3AB	V3C	V2	V3AB	V3C	V2	V3AB	V3C
LB	+0.4	+0.3	+0.2	+2.4	+2.2	+1.5	2.0	1.9	1.9	12.2	11.9	11.9
AR	-0.1	-0.1	≈ 0	-0.6	-0.7	≈ 0	1.7	1.7	1.7	8.5	10.5	10.0
RC	-	+0.3	+0.4	-	+1.8	+2.4	-	1.8	1.8	-	12.2	12.1
ZU	-	+0.1	+0.2	-	+0.7	+1.1	-	1.9	1.8	-	13.1	11.0
LE	-	-0.1	-0.2	-	-0.4	-1.4	-	2.1	1.7	-	12.2	10.1
TA	-	+0.3	-0.1	-	+1.8	-0.5	-	2.1	1.9	-	13.6	11.6
PP	-	-	≈ 0	-	-	-0.3	-	2.2	1.8	-	-	10.8
mean		**+0.1**	**+0.1**	**-**	**+0.9**	**+0.4**	**-**	**2.2**	**1.8**	**-**	**12.5**	**11.1**
stdev		**0.2**	**0.2**	**-**	**1.2**	**1.3**	**-**	**0.2**	**0.1**	**-**	**1.1**	**0.8**

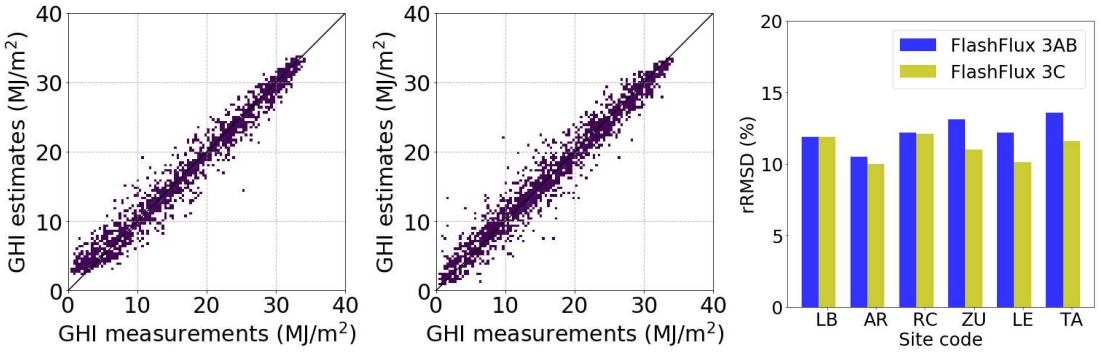

(a) CAMS estimates (AR site) **(b) NASA estimates (AR site)** **(c) FLASHFlux comparison**

Fig. 1: Performance analysis of the models against reference ground measurements.

To obtain a better understanding about the performance characteristics of each model, a discrimination of days based on the predominant daily sky condition is made by using the daily clearness index, K_T. This index is the normalization of the daily GHI, H_h, by the daily irradiation at a horizontal plane in the top of the atmosphere, H_{oh}, so that $K_T = H_h / H_{oh}$ (Duffie and Beckman, 2006). The days are classified into three categories: (i) mostly clear sky ($K_T > 0.65$), (ii) partly cloudy ($0.35 < K_T \leq 0.65$) and (iii) cloudy ($K_T \leq 0.35$). Tab. 4 shows the performance of the CAMS and NASA models when using this classification. It is observed that both models present significant better results for condition (i) days, with a rMBD approximately of -3% and a rRMSD around 5%. For this type of days both models have a negative bias observed in all stations. This is confirmed by the scatter plot of Fig. 2 (a), which shows more samples below the line of perfect agreement (straight line $x = y$). Although the performance of both models is similar under condition (i), overall, the CAMS estimates present better performance, achieving a lower rMBD and rRMSD than the NASA estimates. Relative metrics downgrades as the cloudiness levels increase, firstly because the absolute deviations are higher, but also because

the average value decreases (the normalization value). For partly cloudy days the absolute MBD is reduced in comparison to mostly clear sky days, but the improvement in the relative terms (rMBD) is not such high. An overestimating bias is observed for NASA estimates under this condition and not for CAMS estimates, which exhibit a mixed situation. It can be observed in Fig. 2 (b) than the NASA estimates are, on average, above than CAMS estimates for this kind of days, explaining the different MBD trend. The RMSD for condition (ii) days is higher than for condition (i) days, being the rRMSD significantly higher: the rRMSD increases from 4.8% to 10.6% for the CAMS estimates and from 5.2% to 14.0% for the NASA estimates. Again, an overall better performance of the CAMS model is observed and the differences between models are more important. Finally, for cloudy days both models present the highest metrics, showing overestimating biases and high RMSD values (2.3MJ/m^2 in absolute terms, resulting in ≈42% in relative terms). Overall, the rMBD is higher for the CAMS estimates than for the NASA estimates, but the opposite occurs for the rRMSD. The performance of both models is similar under cloudy conditions, but as the rRMSD is similar (42±0.5%) and the rMBD is lower for NASA than for CAMS (+19% in comparison with +27%), it can be fairly said that NASA model is preferable in this situation. Same conclusion can be obtained by inspecting Fig. 2 (c).

Tab. 4: Performance indicators for the CAMS and NASA models estimate on a daily basis and different type of days.

	Days	**MBD (MJ/m^2)**		**rMBD (%)**		**RMSD (MJ/m^2)**		**rRMSD (%)**	
		CAMS	NASA	CAMS	NASA	CAMS	NASA	CAMS	NASA
Clear sky									
LB	1077	-0.8	-0.5	-3.5	-2.4	1.2	1.1	5.3	4.7
AR	968	-0.4	-0.8	-1.7	-3.0	1.0	1.2	4.2	5.0
RC	427	+0.6	-0.6	-2.7	-2.5	1.0	1.1	4.4	4.6
ZU	547	-0.9	-0.7	-4.0	-3.1	1.4	1.3	6.2	5.8
LE	467	-1.0	-0.9	-4.2	-3.9	1.4	1.3	5.8	5.6
TA	455	-0.5	-0.8	-2.1	-3.4	0.9	1.4	3.9	5.8
PP	298	-0.5	-0.8	-1.9	-3.3	0.9	1.3	3.6	5.2
mean	**-**	**-0.7**	**-0.7**	**-2.9**	**-3.1**	**1.1**	**1.2**	**4.8**	**5.2**
stdev	**-**	**0.2**	**0.1**	**1.0**	**0.5**	**0.2**	**0.1**	**1.0**	**0.5**
Partly Cloudy									
LB	1106	-0.4	+0.7	-2.5	+4.9	1.6	2.2	10.9	10.7
AR	735	-0.4	+0.2	-2.4	+1.2	1.8	2.0	10.8	12.5
RC	550	+0.3	+0.6	+1.9	+4.1	1.6	2.1	10.7	14.0
ZU	445	-0.3	+0.6	-1.7	+4.3	1.7	2.4	11.0	15.6
LE	339	-0.8	+0.1	-4.7	+0.5	1.8	2.3	10.9	14.3
TA	417	-0.1	+0.2	-0.8	+1.4	1.7	2.2	10.4	13.5
PP	324	+0.1	+0.1	+0.3	+0.4	1.6	2.3	9.4	13.2
mean	**-**	**-0.2**	**+0.4**	**-1.4**	**+2.4**	**1.7**	**2.2**	**10.6**	**14.0**
stdev	**-**	**0.4**	**0.3**	**2.1**	**1.9**	**0.1**	**0.1**	**0.6**	**1.0**
Cloudy									
LB	558	+1.2	+1.3	+21.7	+23.1	2.0	2.5	35.8	46.5
AR	450	+1.4	+0.8	+23.0	+13.5	2.2	2.3	37.8	39.1

RC	300	+1.6	+1.0	+29.0	+18.8	2.4	2.3	43.9	41.6
ZU	276	+1.7	+1.0	+31.3	+19.3	2.4	2.3	46.6	43.4
LE	251	+1.7	+0.9	+30.3	+16.4	2.5	2.0	44.7	37.1
TA	305	+1.6	+1.2	+29.1	+22.4	2.5	2.6	45.6	47.4
PP	174	+1.4	+1.2	+22.9	+19.7	2.1	2.5	36.0	43.2
mean	**-**	**+1.5**	**+1.1**	**+26.8**	**19.0**	**2.3**	**2.4**	**41.5**	**42.6**
stdev	**-**	**0.2**	**0.2**	**4.0**	**3.3**	**0.2**	**0.2**	**4.7**	**3.7**

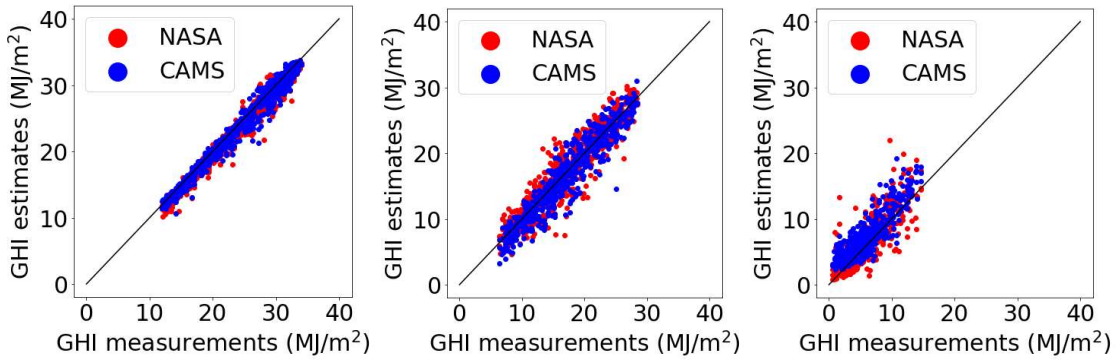

(a) Mostly clear sky days. **(b) Partly cloudy days.** **(c) Cloudy days.**

Fig. 2: Measurements and model's estimates scatter plot for the AR site and each type of day.

The KSI metric provides a different view in the analysis: the statistical dissimilarity. The results are shown in Tab. 5 for all the days (last two columns) and discriminated by type of day. The conclusions are similar to that of the MBD and RMSD analysis but, overall, the NASA model provides a slightly better performance than the CAMS model from the statistical point of view. The KSI of both models is similar under clear sky days. For partly cloudy days the KSI is better for the CAMS estimates and for cloudy days the opposite is observed. The KSI metric for cloudy days is particularly interesting, as can be observed in Fig. 3. In this figure the model's CDF and the measurement's CDF (above) and their absolute difference (below) are shown. The main discrepancy in the model's comparison is the high CDF difference of the CAMS estimates for low irradiation values (cloudy days). This is the same overestimation phenomenon observed in Fig. 3 (c) for this data set. From the KSI perspective this behavior is significant enough to impact the overall rate of the CAMS data set.

Tab. 5: KSI metric (in MJ/m² for the CAMS and NASA models estimates on a daily basis.

Code	Mostly clear sky		Partly cloudy		Cloudy		All days	
	CAMS	NASA	CAMS	NASA	CAMS	NASA	CAMS	NASA
LB	0.8	0.5	0.4	0.8	1.2	1.3	0.5	0.5
AR	0.4	0.7	0.4	0.4	1.4	0.8	0.4	0.3
RC	0.6	0.6	0.3	0.7	1.6	1.1	0.5	0.4
ZU	0.9	0.7	0.3	0.8	1.7	1.0	0.5	0.3
LE	1.0	0.9	0.7	0.3	1.7	0.9	0.8	0.4
TA	0.5	0.8	0.4	0.5	1.6	1.2	0.4	0.4
PP	0.5	0.8	0.4	0.4	1.4	1.2	0.3	0.3
mean	**0.7**	**0.7**	**0.4**	**0.6**	**1.5**	**1.1**	**0.5**	**0.4**
stdev	**0.2**	**0.1**	**0.1**	**0.2**	**0.2**	**0.2**	**0.2**	**0.1**

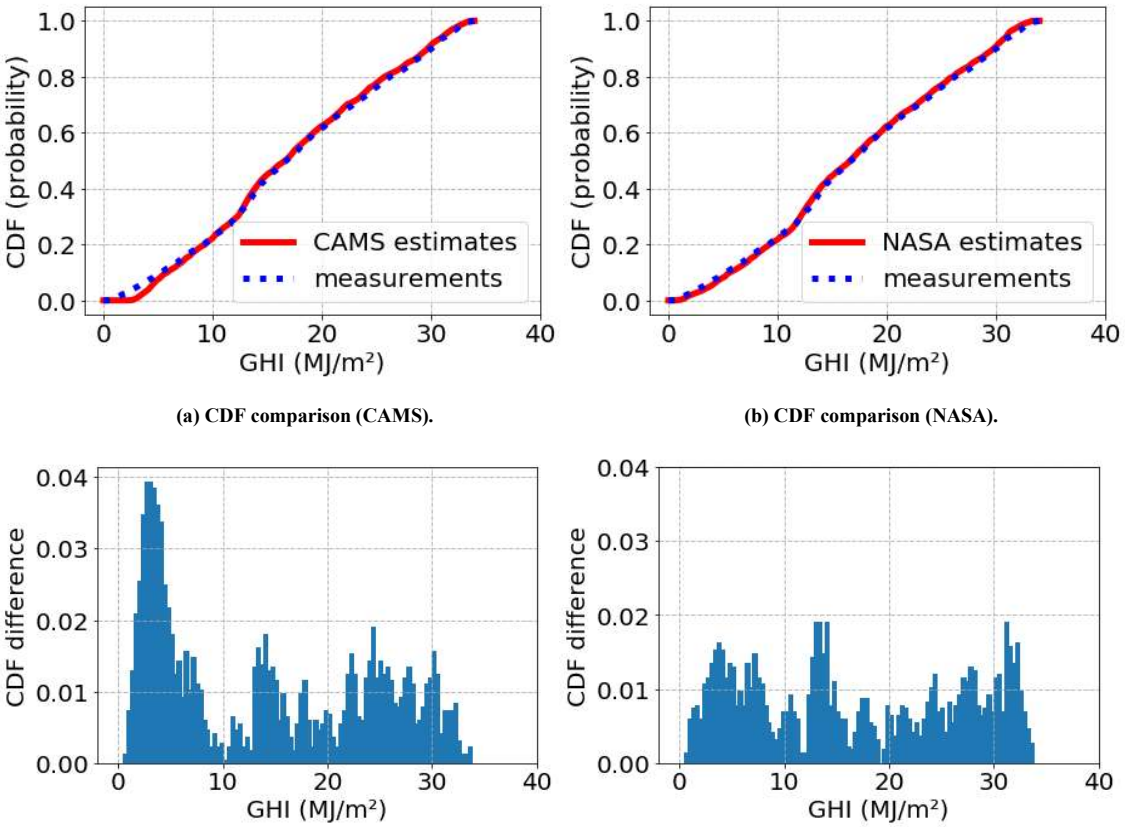

(a) CDF comparison (CAMS).

(b) CDF comparison (NASA).

(c) Absolute CDF difference (CAMS).

(d) Absolute CDF difference (NASA).

Fig. 3: CDF analysis for the AR site: comparison between NASA and CAMS estimates.

5. Conclusions

A performance comparison between the available daily GHI estimates at the CAMS and NASA platforms was done for the region of Uruguay. The assessment was done without any site adaptation technique in order to obtain the end-user uncertainty of the publicly available information. For all sky conditions, it is observed than the CAMS estimates provide a better performance than the NASA estimates (on daily basis). Small biases were found in both estimates, being slightly higher for the NASA estimates. Further, an overestimation trend was found for NASA estimates in the coastal stations affected by their proximity to the Atlantic Ocean, a systematic behavior that is not observed for the CAMS data set. The current version of the NASA's FLASHFlux model (3C) provides better performance for the region than the previous one (3AB). The site average rRMSD is found to be 10.0% for the CAMS estimates and 11.6% for the NASA estimates. From the KSI statistical point of view, the results show a small overall better agreement for the NASA data set. This difference is explained due to an overestimation bias observed for the CAMS data set for low daily irradiation values. In any case, the rRMSD difference between both models is large enough to prefer the CAMS estimates over the NASA estimates for the region.

When discriminating the results by daily sky conditions a systematic underestimation is observed for mostly clear sky days and a systematic overestimation is observed for cloudy days. For the NASA data set the overestimation is also present for partly cloudy days. This is not observed for the CAMS estimates, which exhibit mixed biases for partly cloudy days. The CAMS estimates are preferred for clear sky and partly cloudy days. The difference between models' performance is not high for the former but is significant for the latter. However, for cloudy days, the NASA estimates are preferred, as the CAMS estimates present an important overestimation bias. These conclusions are backed by the MBD/RMSD and KSI analysis.

The uncertainty found in the region for these two models is higher than the one observed for locally-adjusted satellite models based on GOES-East satellite images, like the BDJPT model (Alonso-Suárez et al., 2012), whose rMBD is between ±1.0% and rRMSD is around 7% (on a daily basis against independent data sets, not used for training). The different performance can be explained by the model's local-adaptation and the use of

GOES-East satellite images, which have a smaller pixel size for the region than the MSG satellite. From the end-user perspective, it is preferable to rely on estimates from the previously locally-adapted model (BDJPT) than the publicly available data sets.

6. References

Alonso-Suárez, R., Abal, G., Siri, R., Musé, P., (2012). Brightness-dependent Tarpley model for global solar radiation estimation using GOES satellite images: Application to Uruguay, Solar Energy 86(11):3205--3215.

Alonso-Suárez, R., D'Angelo, M., Abal, G., (2013). Distribución espacial y temporal de la irradiación solar en el Uruguay. Revista Brasileira de Energia Solar 4(2):61--68.

Alonso-Suárez, R. (2017). Estimación del recurso solar en Uruguay mediante imágenes satelitales. Ph.D. thesis Facultad de Ingeniería, Universidad de la República.

Ceballos, J. C., Bottino, M., and de Souza, J. (2004). A simplified physical model for assessing solar radiation over Brazil using GOES 8 visible imagery. Journal of Geophysical Research: Atmospheres, 109(D2).

Cebecauer, T., Súri, M., and Perez, R. (2010). High performance MSG satellite model for operational solar energy applications. In Proceedings of the American Solar Energy Society (ASES), pages 1--5, Phoenix, Arizona, United States.

Duffie, J. and Beckman, W. (2006). Solar Engineering of Thermal Processes. Wiley and Sons, Inc., Hoboken, New Jersey, third edition.

Gurín, M., Cornalino, E., Guggeri, A., Alonso-Suárez, R., Giacosa, G., Abal, G., Terra, R., Chaer, R., (2016). Complementariedad de los recursos renovables (solar--eólico) y su correlación con la demanda de energía eléctrica. Technical Report MIEM-DNE 005-2016, Facultad de Ingeniería, Udelar, Uruguay.

Kratz, D. P., Stackhouse, P. W., Gupta, S. K., Wilber, A. C., Sawaengphokhai, P., McGarragh, G. R. (2014). The Fast Longwave and Shortwave Flux (FLASHFlux) Data Product: Single Scanner Footprint Fluxes. Journal of Applied Meteorology and Climatology, 53(4):1059--1079.

Kriebel, K., Gesell, G., Kästner, M., & Mannstein, H. (2003). The cloud analysis tool APOLLO: Improvements and validations. International Journal of Remote Sensing 24:2389–2408.

Lefèvre, M., Oumbe, A., Blanc, P., Espinar, B., Qu, Z., Wald, L., Homscheidt, M. S., and Arola, A. (2013). McClear: a new model estimating downwelling solar radiation at ground level in clear-sky conditions. Atmospheric Measurement Techniques, European Geosciences Union, 6:2403--2418.

Peel, M. C., Finlayson, B. L., Mcmahon, T. A. (2007). Updated world map of the köppen-geiger climate classification. Hydrology and Earth System Sciences Discussions 11:1633--1644.

Perez, R., Ineichen, P., Moore, K., Kmiecik, M., Chain, C., George, R., and Vignola, F. (2002). A new operational model for satellite-derived irradiances: description and validation. Solar Energy, 73(5):307--317.

Perez, R., Cebecauer, T., and Súri, M. (2013). Chapter 2 - semi-empirical satellite models. In Kleissl, J., editor, Solar Energy Forecasting and Resource Assessment, pages 21--48. Academic Press, Boston..

Qu, Z., Oumbe, A., Blanc, P., Espinar, B., Gesell, G., Gschwind, B., Klüser, L., Lefèvre, M., Saboret, L., Schroedter-Homscheidt, M., and Wald, L. (2017). Fast radiative transfer parameterisation for assessing the surface solar irradiance: The Heliosat-4 method. Meteorologische Zeitschrift, 26(1):33--57.

Rigollier, C., Lefevre, M., and Wald, L. (2004). The method Heliosat-2 for deriving shortwave solar radiation from satellite images. Solar Energy, 77(2):159--169.

Schnitzer, M., Thuman, C., and Johnson, P. (2012). The impact of solar uncertainty on project financeability: mitigating energy risk through on-site monitoring. In Proceedings of the American Solar Energy Society (ASES), pages 1--5, Denver, Colorado, United States.

Vignola, F., Grover, C., Lemon, N., y McMahan, A. (2012). Building a bankable solar radiation dataset. SolarEnergy, 86(8):2218--2229. Progress in Solar Energy 3.